Reprinted from Journal of the Optical Society of America A, Vol. 2, page 1533, September 1985

Simultaneous measurement of spatial-frequency summation and uncertainty effects

Patricia Kramer

Schnurmacher Institute for Vision Research, State College of Optometry, State University of New York, 100 East 24th Street, New York, New York 10010

Norma Graham

Department of Psychology, Columbia University, New York, New York 10027

Dean Yager

Schnurmacher Institute for Vision Research, State College of Optometry, State University of New York, 100 East 24th Street, New York, New York 10010

Received January 18, 1985; accepted May 3, 1985

The predictions for summation and uncertainty effects from several multiple-spatial-frequency-channels models were calculated. The models differed in their assumptions about the shape of the channels' underlying probability-density functions and in the decision rule used to combine the channels' outputs. Varying these assumptions resulted in quite different predictions about the magnitudes of these effects. Simultaneous summation and uncertainty experiments measured the detectability of gratings containing one (simple) or two (compound) spatial frequencies. Performance was assessed in two types of blocks of trials: either each stimulus was in a separate block or three stimuli (two simple gratings and their compound) were randomly intermixed in one block. Quantitative comparisons of the models with the data showed that the increasing-variance Gaussian models (in which the decision variable is the sum of the monitored channels' outputs) provided the best overall fit.

INTRODUCTION

Multiple-spatial-frequency-channels models have been quite successful in quantitatively accounting for the detection of visual patterns.[1–7] For a given stimulus, the magnitude of a channel's output is assumed to vary from trial to trial, and the variability in different channels' outputs is assumed to be probabilistically independent. This assumption of independent variability has been invoked in order to explain several effects, in particular, uncertainty and summation effects. However, the ability of probabilistically independent channels to account quantitatively for these uncertainty and summation effects depends on the precise assumptions of the model, in particular, on the probability-density functions describing the channels' outputs and on the decision rule used for combining the monitored channels' outputs.

Summation Effect (Probability Summation)

The detectability of a compound grating (e.g., a grating containing two far-apart spatial frequencies) is slightly greater than the detectability of either component alone.[3] When the spatial frequencies are far enough apart, no channel will respond to more than one of the spatial frequencies in the compound grating. According to multiple-channels models, the compound grating is more detectable than either simple grating because it affects more than one channel, whereas each component affects only one channel.[8]

The summation effects in the pattern vision literature have been well accounted for by a high-threshold version of a multiple-channels model, usually embodied in the pooling formula suggested by Quick.[3,9] However, high-threshold models predict no uncertainty effect and, therefore, cannot be strictly correct. Further, high-threshold models make incorrect predictions about the psychometric functions for sinusoidal gratings[10] as well as for other stimuli.[11] (See Ref. 12 for a further discussion.)

Uncertainty Effect

Performance when only one simple grating is presented throughout a block of trials (an alone block) is better than performance when trials of two simple gratings (of far-apart spatial frequencies) are randomly presented within a block (an intermixed block). According to multiple-channels models, in an alone block the observer is certain which stimulus will be presented and is assumed to monitor only the one channel sensitive to that stimulus. In an intermixed block the observer is uncertain which stimulus will occur on any given trial and is assumed to monitor the two channels that are sensitive to each of the two simple gratings. The channels that are monitored but are not stimulated on each trial of the intermixed block are assumed to reduce performance (relative to the alone block) by occasionally producing false alarms.[12,13]

The uncertainty effects for spatial frequency and spatial position have been well accounted for by multiple-channels models other than the high-threshold model.[12,13] It is not clear, however, that these other models can simultaneously account for the summation effects.

In this paper, we explore the predictions of several versions of multiple-channels models for both uncertainty and sum-

0740-3232/85/091533-10$02.00

mation effects; six different families of density functions and two combination rules (taking the maximum or the sum of the monitored channels' outputs) are considered. Varying these assumptions about density function and decision rule can make dramatic differences in the predicted magnitudes of the uncertainty and summation effects, although many of these models make quite similar predictions. These predictions are compared with results of simultaneous uncertainty and summation experiments, which measured the detectability of simple and compound gratings. Aside from a small study (600 trials for one observer reported in Ref. 3), this has not been done before to our knowledge. In fact, we are not aware of any such experiment on any sensory dimension. Running uncertainty and summation experiments simultaneously should provide better estimates of the relative magnitudes of these effects for any given observer.

THEORY

Assumptions

(1) *Multiple Channels*
There exist several channels. Each channel is sensitive to a limited range of spatial frequencies. The output of each channel on a particular trial can be represented as a single number; over different trials it can be represented as a random variable.

(2) *Completely Separate Channels*
There is just one channel sensitive to each of the simple gratings, and, if the spatial frequencies of the two gratings are far apart, there is no channel sensitive to more than one of the simple gratings. Also, the only channels sensitive to the compound grating are the two channels that are sensitive to its two components; that is, there are no additional channels that are sensitive to the compound grating.[14]

(3) *Independent Variability*
There is variability across trials in the outputs of a given channel to a given stimulus; therefore the magnitude of that channel's output will have a certain probability density function. The six different families of density functions considered here are illustrated in Fig. 1 and are described below. Furthermore, the outputs of different channels are probabilistically independent.

(4) *Perfect Monitoring*
An observer's response is based only on those channels that are monitored on a particular trial. When an observer knows that any of several spatial frequencies are equally likely to be presented on a given trial, the observer monitors all relevant channels simultaneously. (This implies that the channels' outputs are labeled enough that the observer knows which channel produced which output.) The output of a channel is in no way degraded by increasing the number of monitored channels.

For convenience in later discussions, let M be equal to the number of channels monitored in a block of trials, and let P be equal to the number of channels that are sensitive to a particular stimulus on a given trial.

(5) *Detection Decision Rules*
Two possible assumptions were considered here about how the monitored channels' outputs are combined to lead to an observer's response in a two-interval forced-choice procedure. (One interval contained a blank field and the other interval contained a grating.)

Maximum-Output Rule. The observer chooses the interval that contained the maximum output from all monitored channels.

Sum-of-Outputs Rule. The observer sums the channels' outputs from interval one and sums the channels' outputs from interval two. The observer chooses the interval that contained the larger sum.

The observer uses the same decision rule in all experimental conditions (alone and intermixed blocks of trials).

Probability Density Functions

The six families of density functions are illustrated in Fig. 1. The magnitude of a single channel's output is plotted along the horizontal axis, and probability density is plotted along the vertical axis. Each row shows two functions for a particular family. The function on the left (noise-density function) describes the channel's output when it is not stimulated, that is, when there is a blank field or a stimulus to which that channel is not sensitive. The function on the right (signal-density function) describes the channel's output when it is stimulated (for a particular signal strength). The greater the signal strength, the greater the separation between the noise and signal density functions. Further details of Fig. 1 are given below in the description of each family.

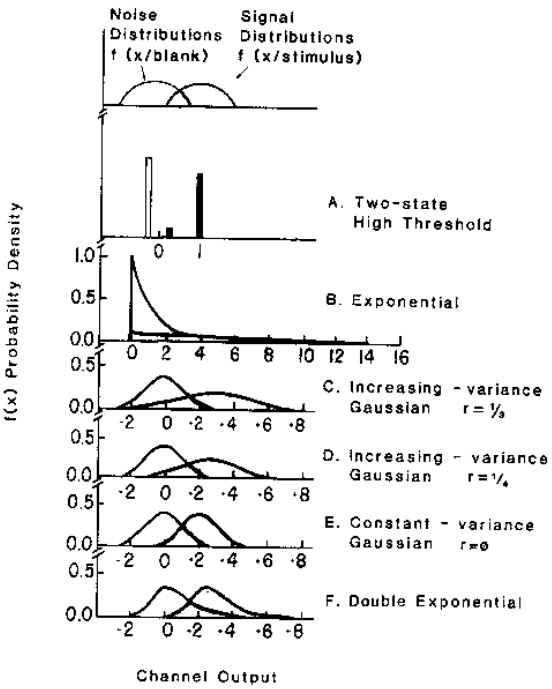

Fig. 1. Six families of probability-density functions. For each family, the probability density for the noise (unshaded) and one signal (shaded) density function are plotted as a function of a channel's output. For the high-threshold family, the noise-density function and the part of the signal-density function near zero are exactly overlapping; they have been offset from zero for clarity.

These families were chosen because they are representative of those commonly used in the literature;[11,15–17] in particular, they are an extension of those used by Davis *et al.*[12] and Yager *et al.*[13] for uncertainty experiments in detection and identification. In fact, the magnitudes of the summation and uncertainty effects predicted by these models span the ranges that have been found empirically; the models range from one that predicts no uncertainty effect but a large summation effect to one that predicts no summation effect but a large uncertainty effect.

High Threshold

The high-threshold family is shown in row A. of Fig. 1. The noise-density function is a uniform function over a small region of output magnitudes near zero. The signal-density function is uniform over this same range (but smaller area) and is also uniform over a small range of values near 1. As the signal strength increases, the area of the signal-density function in the range near one also increases.[18]

Exponential

The exponential family is shown in row B. of Fig. 1. The density functions are zero for output magnitudes less than zero and are equal to $k[\exp(-kz)]$ for output magnitudes (z) greater than or equal to zero, where $k \leq 1$. The value of the signal strength parameter k is inversely proportional to the sensitivity of a channel to a stimulus; as signal strength increases, k decreases.

Gaussian

Three versions of Gaussian families are shown in rows C., D., and E. of Fig. 1. If μ_s and μ_n are the means and if σ_s and σ_n are the standard deviations of the signal- and noise-density functions, respectively, then

$$\frac{\sigma_s}{\sigma_n} = 1 + r\left[\frac{(\mu_s - \mu_n)}{\sigma_n}\right].$$

The value of r determines the rate at which the variance increases as the mean increases and equals 1/3, 1/4, and 0 for rows C., D., and E., respectively. The constant-variance Gaussian family (row E., often called equal variance) is commonly used in the literature; the increasing-variance Gaussians (rows C. and D.) predict receiver-operating-characteristic (ROC) curves whose slopes are similar to those found empirically.[11,20]

Double Exponential

This family is shown in row F. of Fig. 1. Their density functions are described as follows:

$$\exp(-z + U)\{\exp[-\exp(-z + U)]\}.$$

The value of the signal strength parameter U equals zero for the noise-density function and is greater than zero for the signal-density functions. Under certain conditions, the double-exponential model is equivalent to Luce's Choice Theory.[21]

Ten Distinct Models

For the high-threshold model, the sum-of-outputs rule makes exactly the same predictions as the maximum-output rule. For the double exponential, the work involved in computing the sum-of-outputs predictions was greater than seemed worthwhile, so only the maximum-output rule predictions are shown. For the other four distributions, however, predictions for both the sum-of-outputs rule and the maximum-output rule were computed. Therefore predictions for 11 models, 10 of which are distinct, were calculated.

METHODS

The detectability of gratings containing one (simple) or two (compound) spatial frequencies was measured in two types of blocks, using a two-interval forced-choice procedure. In the alone blocks, only one stimulus (either a simple or a compound grating) was presented throughout the block, so the observer was certain which stimulus would be presented on every trial. In the intermixed blocks, trials of three different stimuli (two simple gratings and their compound) were randomly presented, so the observer could not know which stimulus would be presented on any given trial.

Stimuli

The stimuli were vertically oriented sinusoidal gratings produced on the face of an oscilloscope using a conventional z-axis modulation technique.[22] The oscilloscope had a P31 phosphor and a mean luminance of 1.9 fL; it subtended 5.25 deg horizontally and 4 deg vertically. A 12.5-deg circular surround was used, which approximately matched the cathode-ray tube (CRT) in hue and brightness.

The duration of each interval of the two-interval forced-choice procedure was 150 msec; the intervals were separated by 150 msec. An auditory cue was coincident with each interval on each trial. A patterned stimulus, which was temporally gated with an abrupt onset and offset, was presented in one interval; a blank stimulus was presented in the other. Whenever a patterned stimulus was not present, the screen was uniformly illuminated at the same mean luminance as the pattern's.

Spatial Frequencies

In each of the nine experiments, spatial frequencies were chosen to be at least 1 octave apart in order to stimulate separate channels.[6,13] In seven of the nine experiments, a set of two spatial frequencies was used. In two of the nine experiments, a set of three spatial frequencies was used, but only the three possible pairs of spatial frequencies were directly compared. Thus there was a total of thirteen pairings for these experiments. The spatial frequencies were (1 and 4) or (1, 3, and 6) cycles per degree (cpd) for observer PK; (1 and 4), (1 and 16), (4 and 16), (3 and 18) or (3, 9, and 18) cpd for observer CC; (1 and 6) cpd for observer DT; (3 and 18) cpd for observer MB.

Contrasts

The contrasts of the spatial frequencies were chosen before the running of an experiment. For a given observer in a given experiment, the contrasts for the simple gratings were set at values that yielded approximately equal detectability in the alone blocks. For different experiments, however, that particular detectability level was varied in order to get a range of performance levels. Compound gratings had components of the same contrast as the simple gratings.

Phase

The phase of each spatial frequency was varied randomly from trial to trial to prevent observers from utilizing any local cues in the task. Thus the phase of each spatial frequency in the compound grating was varied independently.

Procedure

The observer initiated a trial by pressing a button and made a detection response by indicating the interval in which he or she thought a patterned stimulus appeared.

Five sessions were run for each experiment. A session was composed of an alone and an intermixed condition; generally, one session was run per day. In the alone condition, each stimulus was presented in a separate block of trials; there were 75 trials in each block. In the seven experiments with two spatial frequencies in a set, the alone condition contained three blocks, one for each simple grating (*simple-alone* trials) and one for the compound grating (*compound-alone* trials). In the two experiments with three spatial frequencies in a set, an alone condition contained six blocks, one for each of the three simple and each of the three compound gratings.

In an intermixed condition, trials of two simple gratings (*simple-intermixed* trials) and their compound (*compound-intermixed* trials) were randomly presented within one block. Each stimulus was presented 75 times, for a total of 225 trials per block. In the seven experiments with two frequencies per set, an intermixed condition contained one block; in the other two experiments, an intermixed condition contained three blocks, one for each of the three possible pairs of spatial frequencies. The order of presentation of each of the alone and intermixed blocks was random.

Before each block, 10 practice trials of each stimulus that could appear in that block were presented. These practice trials were identical to the experimental trials but were not included in the data analysis.

To investigate the effects of feedback, feedback was used in four of these nine experiments. As there were no systematic differences in the magnitudes of the summation and uncertainty effects in those experiments that used feedback and those that did not, this manipulation will not be discussed further.

All viewing was binocular with natural pupils. Small vertical lines on the surround above and below the CRT screen served as fixation marks. The observer was instructed to fixate in the middle of these marks.

Session-to-Session Variability

The variability in the data from session to session was somewhat larger than expected if the results from all sessions were random, independent samples from the same population. Therefore, the standard errors calculated from the five sessions were slightly larger than predicted from the binomial distribution ($N = 375$). Calculations showed that they were as large as expected from 190 trials per point (or 380 trials per point in the cases in which performance for the two simple gratings have been averaged).

Observers

Four observers served in these experiments. Three were naive to the purposes of the experiments and had normal or corrected-to-normal visual acuity. The fourth observer was one of the authors (PK) and had a residual visual deficit (20/40).

RESULTS

The empirical and theoretical results have been plotted in the same figures (Figs. 3–6) for ease of comparison. In the next subsection we discuss the empirical results, and in the following subsection we discuss the theoretical results and the comparison with the data.

Empirical Results

In order to compare the relative magnitudes of the summation and uncertainty effects, representative results from one of the thirteen pairings of spatial frequencies are shown in Fig. 2 (3 and 18 cpd for observer CC). The three types of stimuli are indicated on the horizontal axis. Proportion correct is plotted on the vertical axis. Open symbols are from the alone condition, and closed symbols are from the intermixed condition; there were 375 trials per point. Four types of effects are illustrated: two types of summation effects and two types of uncertainty effects. (The results for all experiments are shown in Figs. 3–6.)

Summation Effects

The *blocked-summation* effect is the amount by which performance for the compound grating in the alone condition (compound-alone trials) is greater than that for the simple gratings in the alone condition (simple-alone trials); e.g., in Fig. 2, the right-hand open symbol versus the left-hand and middle open symbols. (This effect is referred to as blocked summation because trials of each stimulus are presented in separate blocks.) The *intermixed-summation* effect is the amount by which performance for the compound grating in the intermixed condition (compound-intermixed trials) is greater than that for the simple gratings in the intermixed condition (simple-intermixed trials); e.g., in Fig. 2, the right-hand filled symbol versus the left-hand and middle filled symbols. In general, the intermixed-summation effect is greater than the blocked-summation effect.

The blocked-summation and intermixed-summation effects

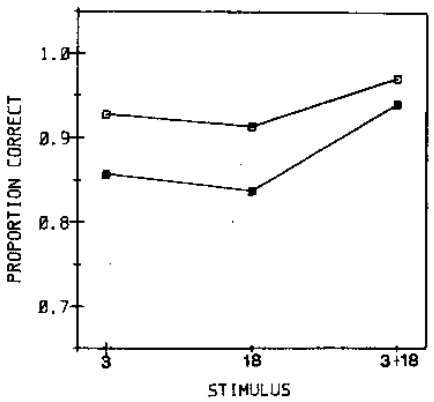

Fig. 2. Results from a representative simultaneous uncertainty and summation experiment. Proportion correct is plotted for three stimuli (3 and 18 cpd and the compound) for alone blocks (open symbols) and intermixed blocks (filled symbols).

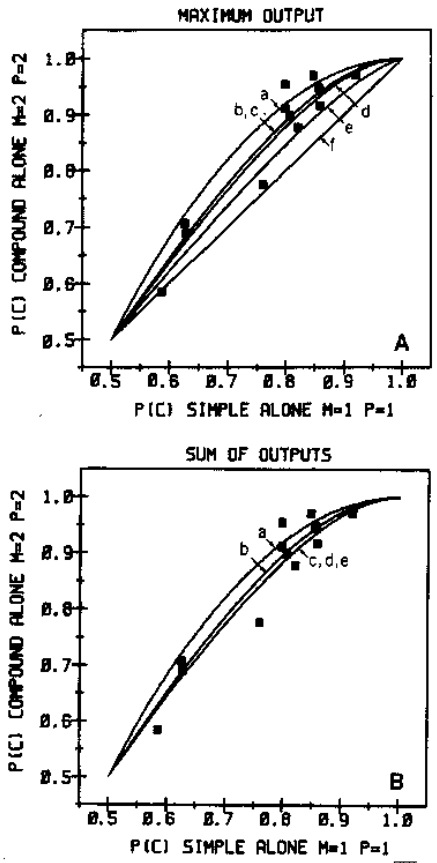

Fig. 3. Blocked-summation effect: empirical results (symbols) and theoretical predictions (curves). Proportion correct for simple-alone trials is plotted against proportion correct for compound-alone trials. A, Theoretical results for the maximum-output rule; B, theoretical results for the sum-of-outputs rule. The curves are labeled as the families of density functions were in Fig. 1.

are summarized for all experiments in Figs. 3 and 4, respectively. (In Figs. 3–5 the data plotted in the top panels have been replotted in the bottom panels. For this subsection, therefore, only the top panels need be referred to. The solid curves are the theoretical predictions and will be discussed in the next subsection.) The average proportion correct for the two simple gratings is plotted along the horizontal axis. The proportion correct for the compound grating is plotted along the vertical axis. The straight line drawn (Fig. 3A, curve f) indicates where the results would lie if there were no summation effects. For both the blocked-summation and the intermixed-summation effects, the proportion correct for the compound grating is always greater than (except for one case where it is equal to) the proportion correct for the simple gratings.

Uncertainty Effects

The *simple-uncertainty* effect is the amount by which performance on simple-intermixed trials is worse than that on simple-alone trials; e.g., in Fig. 2, the left-hand and middle filled symbols versus the left-hand and middle open symbols. The magnitude of the simple-uncertainty effect is like that found previously.[12,13,23] The *compound-uncertainty* effect is the amount by which performance on compound-intermixed trials is worse than that on compound-alone trials; e.g., in Fig. 2, the right-hand filled symbol versus the right-hand open symbol.

The simple-uncertainty effect is summarized for all experiments in Fig. 5. The proportion correct on the simple-alone trials is indicated on the horizontal axis, and the proportion correct on the simple-intermixed trials is indicated on the vertical axis. The straight line drawn (curve a) indicates where the results would lie if there were no effect of uncertainty; all the data points fall below that line.

The compound-uncertainty effect is summarized for all experiments in Fig. 6. The magnitude of this effect is smaller than that of the simple-uncertainty effect; however, even here all but one of the data points fall below the positive diagonal.

Effect of Separation of Frequencies

Olzak and Thomas[24] reported that the amount of summation for a compound grating composed of two spatial frequencies that differ by a factor of 6 (3 and 18 cpd) was less than the amount of summation for a compound grating composed of spatial frequencies that differed by a factor of 2 or 4 (3 and 6 or 3 and 12 cpd). In the present study, the magnitude of the

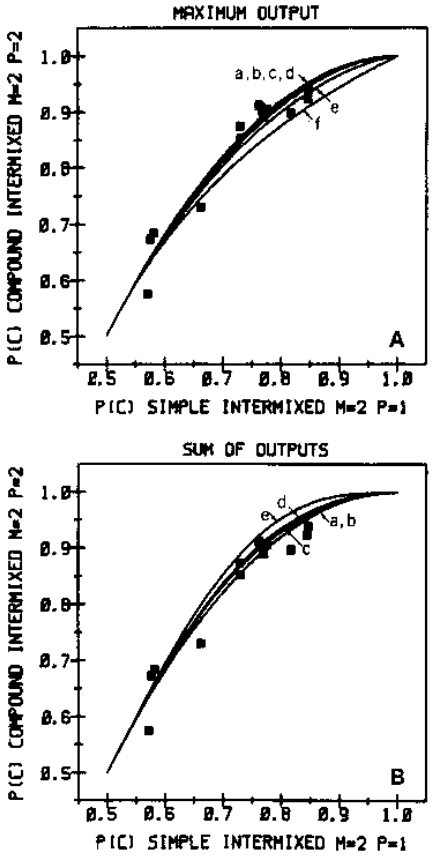

Fig. 4. Intermixed-summation effect: empirical results (symbols) and theoretical predictions (curves). Proportion correct for simple-intermixed trials is plotted against proportion correct for compound-intermixed trials. A, B, and curves as in Fig. 3.

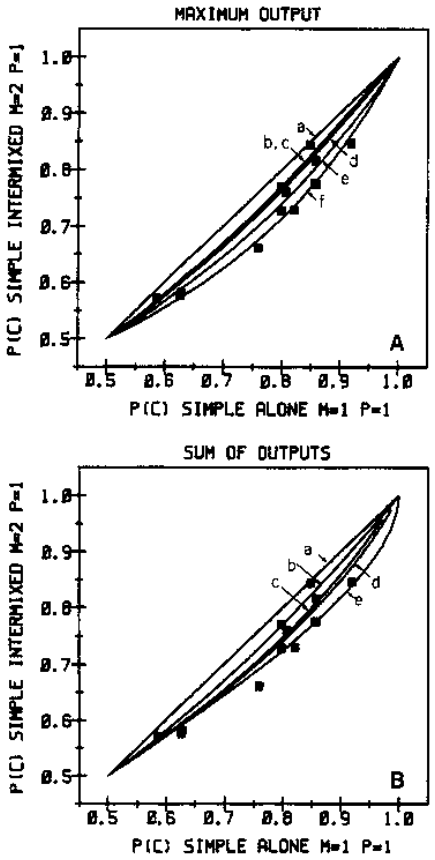

Fig. 5. Simple-uncertainty effect: empirical results (symbols) and theoretical predictions (curves). Proportion correct for simple-alone trials is plotted (horizontal axis) against proportion correct for simple-intermixed trials (vertical axis). A, B, and curves as in Fig. 3.

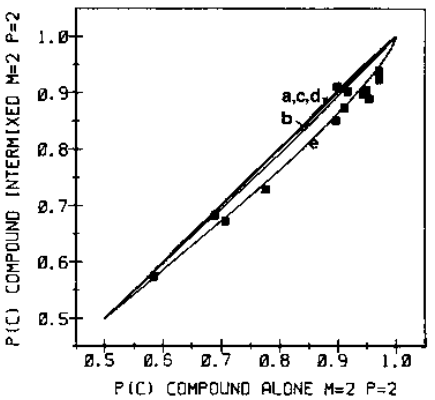

Fig. 6. Compound-uncertainty effect: empirical results (symbols) and theoretical predictions (curves). Empirically, proportion correct for compound-alone trials is plotted against proportion correct for compound-intermixed trials. For each of five families of density functions, the predicted performance for the compound with a sum-of-outputs rule (horizontal axis) is plotted against that with a maximum-output rule (vertical axis).

summation effect for spatial frequencies that differed by a factor of 6 and 16 was compared with that for spatial frequencies that differed by a factor of 2, 3, or 4. There were no systematic differences in the summation results for these two cases.

Theoretical Results and Comparison with Empirical Results

For a given model and signal strength, a predicted ROC curve was generated by computing the hit and false-alarm rates for each type of trial: simple-alone; simple-intermixed; compound-alone; and compound-intermixed. The predicted proportion correct in two-interval forced choice is the area under that ROC curve.[11] The predicted performance in one type of trial was then plotted against predicted performance in another type. By using this procedure for all models and various signal strengths, the theoretical curves shown in Figs. 3–5 were generated. Figures 3A, 4A, and 5A give the predictions for the maximum-output rule, and Figs. 3B, 4B, and 5B give the predictions for the sum-of-outputs rule; the curves are labeled as the families of density functions were in Fig. 1. (See Refs. 13 and 25 for more details.)

Monitoring More Than One Channel: Effect of Density Function

When the observer monitors more than one channel, as in the case of the intermixed and the compound-alone blocks, there are always two consequences—extra hits and extra false alarms—relative to when an observer monitors only one channel as in the simple-alone blocks. Briefly, an uncertainty effect is predicted by these models whenever the harmful effects of extra false alarms outweigh the helpful effects of extra hits. Similarly, summation effects are predicted whenever the helpful effects of extra hits outweight the harmful effects of extra false alarms. (See Refs. 19 and 25 for more details.)

Models with shallow ROC curves predict larger summation effects and smaller uncertainty effects than do models with steep ROC curves.[19,26] The families of density functions were

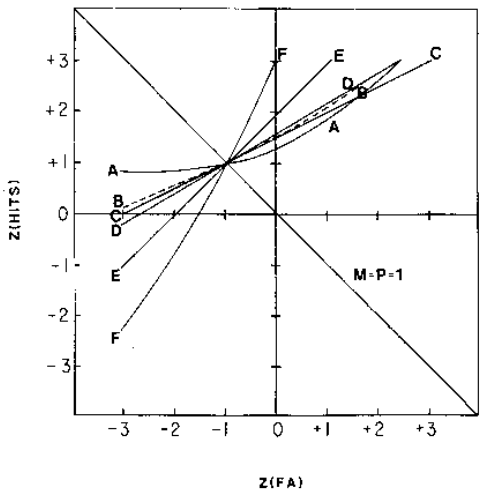

Fig. 7. ROC curves. The ROC curve is shown for each of the six pairs of density functions in Fig. 1. The Z score of a hit is plotted against the Z score of a false alarm.

Table 1. Summary of Models' Fit to Data[a]

	Model	Simple Uncertainty	Blocked Summation	Intermixed Summation
A.	High-threshold	0**	2**	7+
B.	Maximum-exponential	2**	7+	7+
C.	Maximum-Gaussian $R = 1/3$	2**	7+	8+
D.	Maximum-Gaussian $R = 1/4$	3*	8+	8+
E.	Maximum-Gaussian $R = 0$	5+	11**	9
F.	Maximum-double-exponential	10*	12**	11**
B.	Sum-of-exponentials	3*	5+	7+
C.	Sum-of-Gaussians $R = 1/3$	5+	8+	5+
D.	Sum-of-Gaussians $R = 1/4$	5+	8+	5+
E.	Sum-of-Gaussians $R = 0$	9	8+	2**

[a] The leftmost column lists the models. The letters next to the names of the models correspond to those in the figures. The other three columns give the number of data points that fell above each theoretical curve for the simple-uncertainty, blocked-summation, and intermixed-summation effects. Models that can account for the data are indicated by a plus (+). Models that are rejected by a sign-test ($n = 13$) are indicated by one ($p = 0.07$) or two ($p \leq 0.019$) asterisks.

ordered in Fig. 1 according to the slopes of their ROC curves, with the high-threshold model (row A.) having the shallowest slope and the double-exponential model (row F.) having the steepest slope, as illustrated in Fig. 7. Thus the predicted curves in Figs. 3–6 are in the same order as the density functions in Fig. 1. This systematic relationship between ROC slope and the predicted magnitude of these effects can be understood in terms of the trade-off between the extra hits and extra false alarms.[19]

Acceptance-Rejection of Models

Examination of Figs. 3–5 reveals that the magnitude of the blocked-summation, intermixed-summation, and simple-uncertainty effects in these experiments are in the range predicted by the models considered here. (The compound-uncertainty effect is discussed below.) The following paragraphs compare the theoretical predictions with the data; these comparisons are summarized in Table 1. A given model was rejected if the number of the thirteen data points that fell *above* the theoretical curve for that model was less than four or greater than nine. For a two-tailed sign test ($n = 13$), the probability of such an occurrence is less than or equal to 0.07.[27]

Blocked-Summation Effect

The predictions in Fig. 3 compare performance on simple-alone trials—in which the observer is assumed to monitor the one channel sensitive to the one simple grating, $M = 1$ and $P = 1$—with that on compound-alone trials—in which the observer is assumed to monitor the two channels sensitive to each of the components of the compound grating, $M = 2$ and $P = 2$.

Note the orderly relationship in the models' predictions; the high-threshold model (shallow ROC curve) predicts the largest amount of blocked summation, with the other models predicting progressively less (as ROC slope increases). The double exponential (steep ROC curve) with a maximum-output rule predicts no blocked-summation effect.

In accounting for the empirical data (see the summary in Table 1), the high-threshold model (Figs. 3A and 3B, curves a) predicts too much blocked summation. The constant-variance Gaussian and the double exponential with a maximum-output rule (Fig. 3A, curves e and f) predict too little. All the other models predict the appropriate amount of blocked summation: the exponential and increasing-variance Gaussians with either rule (Figs. 3A and 3B, curves b–d) and the constant-variance Gaussian with a sum-of-outputs rule (Fig. 3A, curve e).

Intermixed-Summation Effect

The predictions in Fig. 4 compare performance on simple-intermixed trials—in which the observer is assumed to monitor two channels ($M = 2$), only one of which is sensitive to a simple grating on a given trial ($P = 1$)—with that on compound-intermixed trials—in which the observer monitors two channels ($M = 2$), both of which are sensitive to the compound grating ($P = 2$). All models make very similar predictions for this effect.

The ordering of the models for the maximum-output rule (Fig. 4A) is in the same direction as the blocked-summation results. However, the ordering is reversed for the sum-of-outputs rule (Fig. 4B).

In accounting for the data (see the summary in Table 1), the constant-variance Gaussian with the sum-of-outputs rule (Fig. 4B, curve e) predicts too much intermixed summation, and the double exponential with a maximum-output rule (Fig. 4A, curve f) predicts too little. The constant-variance Gaussian with the maximum-output rule (Fig. 4A, curve e) slightly underpredicts the amount of intermixed summation (with nine points above the curve). The models that predict the appropriate amount of intermixed summation are the high-threshold, the exponential, and the two increasing-variance Gaussians with either rule (Figs. 4A and 4B, curves a–d).

Simple-Uncertainty Effects

The predictions in Fig. 5 compare the performance on simple-alone trials ($M = 1$ and $P = 1$) with that on simple-intermixed trials ($M = 2$ and $P = 1$).

The same type of orderly relationship in the predictions occurs. The high-threshold model (shallow ROC slope) predicts no uncertainty effect. The predicted magnitude of the effect progressively increases (as ROC slope increases), with the largest uncertainty effect predicted by the double exponential (steepest ROC slope).

In accounting for the data (see the summary in Table 1), the high-threshold and exponential models with either rule (Figs. 5A and 5B, curves a and b) and the increasing-variance Gaussian models with a maximum-output rule (Fig. 5A, curves c and d) predict too small a simple-uncertainty effect. The double-exponential (Fig. 5A, curve f) predicts too much. The

constant-variance Gaussian with a sum-of-outputs rule (Fig. 5B, curve e) slightly overpredicts the amount of simple uncertainty (with nine points above the line). The constant-variance Gaussian with a maximum-output rule (Fig. 5A, curve e) and the increasing-variance Gaussians with an sum-of-outputs rule (Fig. 5B, curves c and d) predict the right amount of a simple-uncertainty effect.

Compound-Uncertainty Effect

By the assumptions given above, the performance for the compound grating on compound-alone trials should be equal to that on compound-intermixed trials. In both types of block, the number of channels monitored ($M = 2$) and the number of channels sensitive to the compound grating ($P = 2$) are the same, and—by assumption (5)—the same decision rule is used. Therefore none of the models can account for the compound-uncertainty effect, since all models predict that the data should fall on a straight line (Fig. 6, curve a); that is, no compound-uncertainty effect is predicted. (The other solid curves in this figure are discussed below.)

Effect of Combination Rule

The predicted magnitude of simple-uncertainty, blocked-summation, and intermixed-summation effects was somewhat greater with the sum-of-outputs rule than with the maximum-output rule. (Exceptions were the high-threshold model, for which the predictions are identical for the two rules, and the double-exponential model, for which the sum-of-outputs rule was not calculated.)

Another way of looking at this effect of combination rule is useful at this point. First, with most probability distributions, a maximum-output rule predicts better performance on simple gratings in an intermixed block than does a sum-of-outputs rule.[19] In fact, for constant-variance Gaussians, the maximum-output rule has been shown to be almost optimal in the simple-intermixed condition (i.e., nearly identical to the performance of an ideal observer who maximizes likelihood ratios).[15,17]

Second, with most probability distributions, a sum-of-outputs rule predicts better performance on a compound grating than does a maximum-output rule.[19] For constant-variance Gaussians in a blocked-summation experiment, the sum-of-outputs rule is optimal (App. 9-A of Ref. 11).

Modification of the Decision-Rule Assumption

Consider, therefore, the possibility that the observer can use different combination rules in different conditions [a modification of assumption (5)]. Since the better combination rule for the compound grating is the sum-of-outputs rule, the observer ought to use that rule in the compound-alone blocks. The question of which combination rule is better in blocks where both simple and compound gratings are intermixed is more complicated; the maximum-output rule is better for the simple gratings, but the sum-of-outputs rule is better for the compound gratings. Since simple gratings occurred on two thirds of the trials in the intermixed conditions reported here, an observer might well use a maximum-output rule here. This use of different combination rules in different conditions predicts lower performance for the compound grating in the intermixed condition than in the alone condition, that is, a compound-uncertainty effect.

For each of the five families of density functions for which the predictions from both combination rules were calculated, Fig. 6 compares the predicted performance for a compound grating from the sum-of-outputs rule (horizontal axis) with that from the maximum-output rule (vertical axis). The predicted lower performance from using a maximum-output rule relative to a sum-of-outputs rule is the amount by which the predictions fall below the positive diagonal. This effect is relatively small; the high-threshold predicts no difference, and the exponential and the two increasing-variance Gaussians predict a very small difference. However, the constant-variance Gaussian predicts a difference in performance that accounts quite well for the observed compound-uncertainty effect. Furthermore, for the constant-variance Gaussian, use of the maximum-output rule in the intermixed blocks and the sum-of-outputs rule in the compound-alone block will also account rather well for simple-uncertainty, blocked-summation, and intermixed-summation effects (see Table 1).

DISCUSSION

Using the original assumptions, of the ten models considered, the two increasing-variance Gaussians with a sum-of-outputs rule provided the best overall fit, accounting for the simple-uncertainty, blocked-summation, and intermixed-summation results. None of the original models was able to account for the compound-uncertainty effect. However, a constant-variance Gaussian model in which a sum-of-outputs rule is used in compound-alone blocks and a maximum-output rule is used in intermixed blocks can account for all four effects.

Comparisons with Previous Uncertainty Results

The results of previous simple-uncertainty experiments are in agreement with the results reported here.[12,13,28] In all these studies, when the number of alternative stimuli increases from *one* to a higher number, the size of the uncertainty effect is in the range predicted by the following four models: the constant-variance Gaussian with a maximum-output rule, either increasing-variance Gaussian with a sum-of-outputs rule, and the constant-variance Gaussian with a sum-of-outputs rule. These four models predict the largest uncertainty effects, with the exception of the double-exponential with the maximum-output rule.

However, Yager *et al.*[13] have also shown that when the number of alternative stimuli goes from *two* to a higher number, the uncertainty effects for either detection or identification are too small to be predicted by the above four models. Rather, these effects are in the range predicted by the following four models: the exponential with the maximum-output rule, the exponential with the sum-of-outputs rule, and both increasing-variance Gaussians with the maximum-output rule. These latter four models predict the smallest uncertainty effect, other than the high-threshold which predicts no effect.

The reason for this discrepancy is far from clear. Two possible reasons suggested by Yager *et al.*[13] are ruled out by the results of this study. In Ref. 13 the intermixed and alone conditions were run on alternating days; possibly day-to-day variability accounted for the large decrement going from one to two relative to two to four. In the present study, however, alone and intermixed conditions were run on the same day. In Ref. 13, only detection responses were required by the ob-

server in alone conditions; however, both detection and identification responses were required in the intermixed conditions; perhaps this double response caused the discrepancy in the magnitude of effects. In the present study, only detection responses were ever required. A third possibility that they mention—greater criterion variability in the intermixed than in the alone conditions—remains, although they present some evidence against it and it seems unlikely here, where a two-interval forced-choice procedure was used. (Yager *et al.* used a single-interval yes–no procedure.)

Another intriguing possibility is that as soon as the number of alternative stimuli is greater than one, the observer's uncertainty increases dramatically and thus the observer monitors more additional channels than there are additional alternative stimuli. When the number of alternatives increases from two (thus the observer is already monitoring more than one channel) to a higher number, however, the observer will monitor only as many additional channels as there are additional alternative stimuli. This discrepancy deserves further study.

Intrinsic Uncertainty

The models tested here considered only *extrinsic* uncertainty, arising from the number of alternative stimuli in a given set. The observer was assumed to ignore perfectly all irrelevant sources of information, that is, all irrelevant channels. To the extent that the observer does not ignore this irrelevant information, it is necessary to incorporate *intrinsic* uncertainty into these models (See Refs. 20 and 29–32 for discussions of intrinsic uncertainty). One way to do this is to let each channel in the above presentation (one channel for each simple stimulus) be a megachannel composed of many microchannels. For a given simple stimulus, the sensitive megachannel will contain some microchannels that are not sensitive to that simple stimulus at all. (These insensitive microchannels reflect the observer's intrinsic uncertainty about which microchannels are relevant.)

For example, let each microchannel be characterized by the constant-variance Gaussian family of density functions. The means of the sensitive microchannels are assumed to be increasing linearly with contrast. The means of the insensitive microchannels are assumed to remain at zero regardless of contrast. Let the megachannel's output be the maximum of the microchannels' outputs; the megachannel's output will have a mean that increases as an accelerating function of contrast and have a variance that also increases. As Pelli[32] shows, such a megachannel can quantitatively account for several important detection results. In particular, it can account for the way in which empirical ROC curves get shallower as detectability increases.

This approach allows us to relate others' work on intrinsic uncertainty to our own on extrinsic uncertainty. The exponential and increasing-variance Gaussian families also predict ROC slopes like those found empirically.[11,20] Further, the ROC slope is a primary determinant of the multiple-channels models' predictions for uncertainty and summation experiments.[19,25] Therefore a multiple-channels model [assumptions (1)–(5) for exponential and increasing-variance Gaussian density functions] in which a channel is a megachannel like that described in the preceding paragraphs would predict uncertainty and summation effects like those shown in Figs. 3–5.

Comparisons with Previous Summation Results

One summation result of the present study that is not in agreement with previous findings[24] is that the amount of summation for a compound stimulus did not depend upon the separation of spatial frequencies comprising the compound.

Two results are in agreement with previous studies. First, although there have been no quantitative comparisons of models in predicting blocked or intermixed-summation effects, previous studies have found that the intermixed-summation effect is well predicted by the high-threshold model and is in agreement with the results found here.[3] Second, a comparison across previous studies shows that the blocked-summation effect is smaller than the intermixed-summation effect (e.g., compare the results of Graham and Nachmias[33] with those of Graham *et al.*[3]).

Viability of the Quick Pooling Model

The success of the Quick pooling model in predicting pattern thresholds seems to rest with the fact that it has been employed in intermixed-summation experiments. All 10 models considered here make remarkably similar predictions for the magnitude of this effect. That is, the predicted magnitude of an intermixed-summation effect *does not depend* on either probability density function or combination rule. (This similarity in the models' predictions also holds when the compound contains four components.[19,25]) Therefore, even though the Quick pooling model is clearly wrong, since it predicts no uncertainty effect and too much blocked-summation effect, it is a viable predictor of an intermixed-summation effect.

ACKNOWLEDGMENTS

The authors thank Jacob Nachmias for many helpful discussions during the course of this research and Elizabeth T. Davis, Ronald Growney, Lynn A. Olzak, Denis Pelli, and an anonymous reviewer for their comments on an earlier draft of this paper. This work was done in partial fulfillment of requirements for the Ph.D. degree awarded to Patricia Kramer; portions of this work were presented at the 1984 Annual Meeting of the Optical Society of America and the 1985 Annual Meeting of the Association for Research in Vision and Ophthalmology. This research was funded in part by National Science Foundation grant BNS-83-11350 to Dean Yager.

REFERENCES

1. J. R. Bergen, H. R. Wilson, and J. D. Cowan, "Further evidence for four mechanisms mediating vision at threshold: sensitivities to complex gratings and aperiodic stimuli," J. Opt. Soc. Am. **69**, 1580–1586 (1979).
2. N. Graham, "Visual detection of aperiodic spatial stimuli by probability summation among narrow band channels," Vision Res. **17**, 637–652 (1977).
3. N. Graham, J. G. Robson, and J. Nachmias, "Grating summation in fovea and periphery," Vision Res. **18**, 815–826 (1978).
4. H. Mostafavi and D. J. Sakrison, "Structure and properties of a single channel in the human visual system," Vision Res. **16**, 957–968 (1976).
5. R. F. Quick, W. W. Mullins, and T. A. Reichert, "Spatial summation effects on two-component grating thresholds," J. Opt. Soc. Am. **68**, 116–121 (1978).
6. J. P. Thomas, J. Gille, and R. A. Barker, "Simultaneous visual

detection and identification: data and theory," J. Opt. Soc. Am. **72,** 1642–1641 (1982).
7. A. B. Watson, "Summation of grating patches indicates many types of detector at one retinal location," Vision Res. **22,** 17–26 (1982).
8. M. B. Sachs, J. Nachmias, and J. G. Robson, "Spatial frequency channels in human vision," J. Opt. Soc. Am. **61,** 1176–1186 (1971).
9. R. F. Quick, "A vector magnitude model of contrast detection," Kybernetic **16,** 65–67 (1974).
10. J. Nachmias, "On the psychometric function for contrast detection," Vision Res. **21,** 215–233 (1981).
11. D. M. Green and J. A. Swets, *Signal Detection Theory and Psychophysics* (Wiley, New York, 1974).
12. E. T. Davis, P. Kramer, and N. Graham, "Uncertainty about spatial frequency, spatial position, or contrast of visual patterns," Percept. Psychophys. **33,** 20–28 (1983).
13. D. Yager, P. Kramer, M. Shaw, and N. Graham, "Detection and identification of spatial frequency: models and data," Vision Res. **24,** 1021–1035 (1984).
14. However, the theoretical results presented here can be straightforwardly applied to the case in which more than one channel is sensitive to each simple grating (but no individual channel is sensitive to more than one of the simple gratings) by assuming that the outputs from all the channels sensitive to a simple grating are combined in some manner and then treating the combined output as coming from a single channel.
15. D. M. Green and T. G. Birdsall, "Detection and recognition," Psychol. Rev. **85,** 192–206 (1978).
16. D. M. Green and D. L. Weber, "Detection of temporally uncertain signals," J. Acoust. Soc. Am. **62,** 948–954 (1980).
17. L. W. Nolte and D. Jaarsma, "More on the detection of one of *M* orthogonal signals," J. Acoust. Soc. Am. **41,** 497–505 (1967).
18. Alternatively, one could portray this high-threshold family as infinitely thin (delta) functions. One then needs to expand the detection-decision rule [assumption (5)] to say that when the decision variable has the exact same value in the two intervals, the observer guesses. This version of the model and the one presented in the text make identical predictions (see Ref. 19).
19. N. Graham, P. Kramer, and D. Yager, "Explaining uncertainty effects and probability summation," Invest. Ophthalmol. Vis. Sci. Suppl. **24,** 186 (1983) (manuscript available from P. Kramer).
20. J. Nachmias and E. Kocher, "Visual detection and discrimination of luminance increments," J. Opt. Soc. Am. **60,** 382–389 (1970).
21. J. Yellott, "The relationship between Luce's choice axiom, Thurstone's theory of comparative judgment, and the double-exponential model," J. Math. Psychol. **15,** 109–144 (1977).
22. F. W. Campbell and D. B. Green, "Optical and retinal factors affecting visual resolution," J. Physiol. **18,** 576–593 (1965).
23. E. T. Davis and N. Graham, "Spatial frequency uncertainty effects in the detection of sinusoidal gratings," Vision Res. **21,** 705–712 (1981).
24. L. A. Olzak and J. P. Thomas, "Gratings: why frequency discrimination is sometimes better than detection," J. Opt. Soc. Am. **71,** 64–70 (1981).
25. P. Kramer, "Summation and uncertainty effects in the detection of spatial frequency," Ph.D. dissertation (Columbia University, New York, 1984).
26. The ROC slope is, of course, not the only predictor of the magnitudes of these effects; whenever the ROC curves are not exactly straight lines, they do not have a single slope. However, the ROC curves of the models used here are straight enough to make "slope" a good predictor.
27. Since several of the data points come from the same observer and, in two of the experiments, the results from the simple-alone blocks are compared with more than one of the compound-alone blocks and with more than one intermixed block, these 13 data points are not truly independent. However, this deviation from independence is not great.
28. T. E. Cohn and D. J. Lasley, "Detectability of a luminance increment: effect of spatial uncertainty," J. Opt. Soc. Am. **64,** 1715–1719 (1974).
29. W. P. Tanner, Jr., "Physiological implications of psychophysical data," Ann. N.Y. Acad. Sci. **89,** 752–765 (1961).
30. J. Nachmias, "Signal detection theory and its application to problems in vision," in *Handbook of Sensory Physiology, Vol. VII/4,* D. Jameson and L. Hurvich, eds. (Springer-Verlag, New York, 1972).
31. T. E. Cohn, L. N. Thibos, and R. N. Kleinstein, "Detectability of a luminance increment," J. Opt. Soc. Am. **64,** 1321–1327 (1974).
32. D. G. Pelli, "Uncertainty explains many aspects of visual contrast detection and discrimination," J. Opt. Soc. Am. A **2,** 1508–1532 (1985).
33. N. Graham and J. Nachmias, "Detection of grating patterns containing two spatial frequencies: a comparison of single-channel and multiple-channels models," Vision Res. **11,** 251–259 (1971).